

Geology

Controls on fluvial evacuation of sediment from earthquake-triggered landslides --Manuscript Draft--

Manuscript Number:	G36157R1
Full Title:	Controls on fluvial evacuation of sediment from earthquake-triggered landslides
Short Title:	fluvial residence time of coseismic landslide
Article Type:	Article
Keywords:	Wenchuan earthquake; residence time; landslide; suspended sediment
Corresponding Author:	Zhangdong Jin Institute of Earth Environment, Chinese Academy of Sciences Xi'an, Shaanxi CHINA
Corresponding Author Secondary Information:	
Corresponding Author's Institution:	Institute of Earth Environment, Chinese Academy of Sciences
Corresponding Author's Secondary Institution:	
First Author:	Jin Wang
First Author Secondary Information:	
Order of Authors:	Jin Wang Zhangdong Jin Robert Hilton Fei Zhang Alexander Densmore Gen Li A. Joshua West
Order of Authors Secondary Information:	
Manuscript Region of Origin:	CHINA
Abstract:	<p>Large earthquakes in active mountain belts can trigger landslides which mobilize large volumes of clastic sediment. Delivery of this material to river channels may result in aggradation and flooding, while sediment residing on hillslopes may increase the likelihood of subsequent landslides and debris flows. Despite this recognition, the controls on the residence time of coseismic landslide sediment in river catchments remain poorly understood. Here we assess the residence time of fine-grained (<0.25 mm) landslide sediment mobilized by the 2008 Mw 7.9 Wenchuan earthquake, China, using daily suspended sediment discharge measured in 16 river catchments from 2006 to 2012. Following the earthquake, suspended sediment discharge was elevated 3-7 times compared to 2006-2007. However, the total 2008-2012 export (92.5 ± 9.3 Mt from 68,719 km²) was much less than estimates of fine-grained sediment input by coseismic landslides (418+437/-302 Mt) determined by landslide area-volume scaling and deposit grain-size distributions. We estimate the residence time of fine-grained sediment in the affected river catchments using the post-earthquake rate of sediment export, and find it ranges from one year to over a century. The first-order variability in fine sediment residence time is proportional to the areal extent of coseismic landsliding, and is inversely proportional to the frequency of intense runoff events (>5 mm day⁻¹). Together with previous observations from the 1999 Chi-Chi earthquake in Taiwan, our results demonstrate the importance of landslide density and runoff intensity in setting the duration of earthquake-triggered landslide impacts on river systems.</p>
Response to Reviewers:	

Publisher: GSA
Journal: GEOL: Geology
DOI:10.1130/G36157.1

1 Controls on fluvial evacuation of sediment from
2 earthquake-triggered landslides

3 Jin Wang^{1,2,3}, Zhangdong Jin^{1,4*}, Robert G. Hilton², Fei Zhang¹, Alexander L. Densmore^{2,5},
4 Gen Li⁶, and A. Joshua West⁶

5 ¹*State Key Laboratory of Loess and Quaternary Geology, Institute of Earth Environment, Chinese
6 Academy of Sciences, Xi'an 710075, China*

7 ²*Department of Geography, Durham University, Durham, DH1 3LE, UK*

8 ³*University of Chinese Academy of Sciences, Beijing 100049, China*

9 ⁴*Institute of Global Environmental Change, Xi'an Jiaotong University, Xi'an 710049, China*

10 ⁵*Institute of Hazard, Risk and Resilience, Durham University, Durham, DH1 3LE, UK*

11 ⁶*Department of Earth Sciences, University of Southern California, Los Angeles, California 90089,
12 USA*

13 *E-mail address: zhdjin@ieecas.cn

14 **ABSTRACT**

15 Large earthquakes in active mountain belts can trigger landslides which mobilize large
16 volumes of clastic sediment. Delivery of this material to river channels may result in aggradation
17 and flooding, while sediment residing on hillslopes may increase the likelihood of subsequent
18 landslides and debris flows. Despite this recognition, the controls on the residence time of
19 coseismic landslide sediment in river catchments remain poorly understood. Here we assess the
20 residence time of fine-grained (<0.25 mm) landslide sediment mobilized by the 2008 M_w 7.9

21 Wenchuan earthquake, China, using daily suspended sediment discharge measured in 16 river
22 catchments from 2006 to 2012. Following the earthquake, suspended sediment discharge was
23 elevated 3–7 times compared to 2006–2007. However, the total 2008–2012 export (92.5 ± 9.3 Mt
24 from $68,719 \text{ km}^2$) was much less than estimates of fine-grained sediment input by coseismic
25 landslides ($418+437/-302$ Mt) determined by landslide area-volume scaling and deposit grain-size
26 distributions. We estimate the residence time of fine-grained sediment in the affected river
27 catchments using the post-earthquake rate of sediment export, and find it ranges from one year to
28 over a century. The first-order variability in fine sediment residence time is proportional to the
29 areal extent of coseismic landsliding, and is inversely proportional to the frequency of intense
30 runoff events ($>5 \text{ mm day}^{-1}$). Together with previous observations from the 1999 Chi-Chi
31 earthquake in Taiwan, our results demonstrate the importance of landslide density and runoff
32 intensity in setting the duration of earthquake-triggered landslide impacts on river systems.

33 **INTRODUCTION**

34 Large earthquakes can trigger widespread coseismic landslides which mobilize large
35 volumes of sediment (Keefer, 1984; 1994). Landslide sediment can cause river bed aggradation,
36 increasing the frequency and magnitude of floods (e.g. Korup et al., 2004) and affect water
37 resources and hydro-electric power generation (Glade and Crozier, 2005). Export of sediment
38 mobilized by coseismic landslides also governs the role of earthquakes in landscape evolution
39 (Hovius et al., 2011; Li et al., 2014). Despite this recognition, the timescales over which
40 earthquake-landslide sediment impacts river catchments remain poorly constrained. Examples

41 from Papua New Guinea, New Zealand and Japan have provided estimates of the time required to
42 remove coseismic landslide sediment from catchments, termed here the ‘residence time’, that
43 range from <1 year to >50 years (Pain and Bowler, 1973; Pearce and Watson, 1986; Koi et al.,
44 2008; Howarth et al., 2012). In Taiwan, intense precipitation associated with tropical cyclones
45 after the 1999 M_w 7.6 Chi-Chi earthquake led to greatly enhanced sediment export and the return
46 of suspended sediment loads to pre-earthquake levels within ~6 years (Dadson et al., 2004;
47 Yanites et al., 2010; Hovius et al., 2011; Huang and Montgomery, 2012). However, we lack a
48 holistic view of what controls the residence time of earthquake-mobilized sediment across events
49 and river catchments, necessary to better manage earthquake hazards (Keefer, 1994; Huang and
50 Fan, 2013) and to understand landscape evolution (Li et al., 2014).

51 Here we examine the impact of the 2008 M_w 7.9 Wenchuan earthquake, which triggered
52 more than 57,150 landslides in the Longmen Shan, China (Li et al., 2014), on three major river
53 catchments (Min Jiang, Tuo Jiang, and Fu Jiang) (Fig. 1). The earthquake provides insight due to:
54 i) the large spatial gradients in coseismic landsliding (Li et al., 2014) and ii) the variable climate
55 and therefore the variable sediment transport conditions across the impacted area (Liu-Zeng et al.,
56 2011). These factors allow us to assess the relative importance of sediment supply and fluvial
57 transport capacity in setting the residence time of earthquake-mobilized sediment. The Wenchuan
58 earthquake occurred along the Beichuan and Pengguan faults at the eastern margin of the Tibetan
59 Plateau (Xu et al., 2009), where the regional climate is dominated by the East Asian and Indian
60 summer monsoons. Annual precipitation is 600–1,100 mm yr⁻¹, with 70–80% of rainfall between

61 May and October (Liu-Zeng et al., 2011). Coseismic landslides mobilized $\sim 2.8+0.9/-0.7$ km³ of
62 clastic sediment in the three major river basins (Li et al., 2014). Using a data set of unprecedented
63 temporal resolution, we examine the immediate (daily to weekly) and longer-term (years to
64 decades) impacts of earthquake-triggered landslides on river suspended loads and assess the
65 controls on fine-grained sediment residence time.

66 MATERIALS AND METHODS

67 Daily water discharge (Q_w , m³ s⁻¹) and daily suspended sediment concentration (SSC, mg
68 L⁻¹) were measured at 16 gauging stations of the Chinese Bureau of Hydrology from 2006 to 2012
69 (Table DR1 in the GSA Data Repository¹). Ten stations are located downstream of heavily
70 landslide-impacted areas (Li et al., 2014), where landslide areal density ρ_{ls} (the fraction of area
71 affected by landslide scars) reach $> 1\%$. Six stations have lower ρ_{ls} (Fig. 1). SSC samples were
72 collected up to 8 times per day, depending upon water level variations, with a depth-integrated
73 sampler along 5–10 vertical profiles (Ministry of Water Resources of China, 2007). Samples were
74 filtered through 0.7 μ m paper filters, and the sediment was dried and weighed. The grain size
75 distribution was measured on selected samples. Daily suspended sediment discharge ($SSC \times Q_w$)
76 was summed to quantify annual suspended sediment discharge, Q_{ss} (Mt yr⁻¹). Uncertainties on
77 SSC were estimated using the standard deviation of daily repeat SSC measurements at the
78 Sangping station and were propagated into estimates of Q_{ss} (Table DR2). Before and after the
79 earthquake, 97% of suspended sediment was transported between May and October during
80 monsoonal rainfall (Fig. DR1). During winter, some rivers have very low Q_w and SSC, so 10 of 16

81 stations only measured SSC from April or May to October. Only measured samples were used to
82 quantify annual suspended discharge.

83 Estimates of landslide sediment volume (V_{ls} , m^3) in each catchment were taken from Li et
84 al. (2014), who mapped the areas (A_{ls} , m^2) of coseismic landslides. Total V_{ls} was estimated using a
85 power law relationship between A_{ls} and V_{ls} (Guzzetti et al., 2009; Larsen et al., 2010), with a
86 coefficient (α) and exponent (γ) derived from field measurements of 41 landslides within the
87 Longmen Shan (Parker et al., 2011; Li et al., 2014). The uncertainties on the total volume of the
88 57,150 landslides were determined by Monte Carlo simulation taking errors on α and γ into
89 account (Li et al., 2014). To compare landslide inputs to suspended load Q_{ss} , we used a
90 compilation of grain size measurements from 33 sites across 9 landslide deposits in the major river
91 basins (Table DR3). Across these sites, the average weight percent of material <0.25 mm in
92 diameter was $6.6 \pm 4.4\%$ ($\pm 1\sigma$), which we use to estimate fine sediment volume and its likely
93 variability in the landscape.

94 **FLUVIAL RESPONSE TO THE WENCHUAN EARTHQUAKE**

95 The three major rivers draining the impacted area experienced an increase in Q_{ss} following
96 the earthquake (Fig. 1). At the most downstream gauging stations, post-earthquake Q_{ss} was ~ 3 to
97 ~ 7 times higher than in 2006-2007 (Fig. 1). These increases are similar to those in Taiwan rivers
98 impacted by the 1999 Chi-Chi earthquake (Dadson et al., 2004; Hovius et al., 2011). In contrast to
99 the elevated post-earthquake Q_{ss} values (Fig. 1), changes in annual water discharge were relatively
100 minor (Fig. DR2). The enhanced Q_{ss} is consistent with observations of dilution of ^{10}Be

101 concentrations in detrital quartz in some of the studied catchments (West et al., 2014). Input of
102 ^{10}Be -depleted landslide material is thought to be responsible for a decrease in detrital ^{10}Be of river
103 sediments (0.25-1 mm) and suggest that sediment discharge increased ~2 to ~9 times in the 2 years
104 following the earthquake (West et al., 2014).

105 The daily measurements also reveal the immediate fluvial response to the earthquake and
106 its aftershocks. At Sangping station on the Zagunao River (drainage area 4,600 km², ρ_{ls} ~0.3%;
107 Table DR1), SSC 18 h after the earthquake (1,532 mg L⁻¹) was 57 times higher than that measured
108 6 h before the earthquake (27 mg L⁻¹), while Q_w remained roughly constant (Fig. 2A). This
109 immediate response is consistent with delivery of some fine-grained coseismic landslide sediment
110 directly to rivers. SSC then decreased over ~10 days while Q_w was relatively invariant, indicating
111 removal of available sediment from the banks and bed of the active river channel (Fig. 2A).

112 Three measurements depart significantly from this pattern (Fig. 2A). First, higher SSC
113 values on 14/05/2008 (1,756 mg L⁻¹) and 15/05/2008 (2,652 mg L⁻¹) were measured within 24 h of
114 the first large aftershock occurred within 20 km of the gauging station (M_w 5.4, 10:54 on
115 14/05/2008; USGS, 2013). Then, SSC doubled (from 796 to 1,347 mg L⁻¹) between 08:00 and
116 20:00 on 16/05/2008, coincident with an M_w 5.6 aftershock (13:26 on 16/05/2008; USGS, 2013)
117 which occurred 26 km from the station. We tentatively link these aftershocks to the further supply
118 of fine-grained sediment to the river channel, through either new landslides or remobilization of
119 loose material.

120 The Q_{ss} at Sangping over the 10 days following the earthquake (Fig. 2A) was 0.09 ± 0.02
121 Mt, much less than the estimated fine-grained landslide inputs of 10+12/-8 Mt upstream of the
122 station. Therefore, to elucidate the longer-term pattern of sediment export, we use two sets of
123 nested gauging stations upstream and downstream of the landslide-affected area (Fig. 1). To
124 average over short-term variability (e.g. Fig. 2A), we sum Q_{ss} over half-year time intervals and
125 calculate the 'downstream sediment gain', the ratio of downstream to upstream Q_{ss} . After the
126 earthquake, downstream sediment gain increased by ~4 times in the Zagunao River along a 55 km
127 reach with $\rho_{ls} \sim 0.3\%$ (Fig. 2B), and increased by ~12 times in the Fu Jiang along a 105 km reach
128 with $\rho_{ls} \sim 0.6\%$ (Fig. 2C). In both locations, downstream water gain showed no change after the
129 earthquake (Fig. DR3).

130 Post-earthquake decline in the downstream sediment gain for the Fu Jiang can be described
131 by a power-law function of time ($r^2 = 0.94$) (Fig. 2C). This declining trend suggests that the
132 suspended sediment loads would return to pre-earthquake levels in 6 ± 1 years, similar to estimates
133 following the Chi-Chi earthquake in Taiwan (Hovius et al., 2011). In contrast, in the Zagunao
134 River the post-earthquake decline in downstream sediment gain within the 4 years of our data set is
135 less clear (Fig. 2B). In this case, a power-law curve does not describe the trend well ($r^2 = 0.39$), and
136 the data suggest that elevated suspended load may persist for longer than in the Fu Jiang. To better
137 understand the fluvial response to the earthquake, we examine all catchments in the Longmen
138 Shan and consider both the coseismic landslide sediment input and the climatic setting of each
139 basin.

140 **RESIDENCE TIME OF EARTHQUAKE-MOBILIZED SEDIMENT**

141 Over the Longmen Shan, the mean annual Q_{ss} following the earthquake (2008–2012) was
142 $18.5 \pm 7.4 \text{ Mt yr}^{-1}$ ($\pm 1\sigma$). Deducting an estimate of the background Q_{ss} (2006–2007, $4.2 \pm 2.6 \text{ Mt}$
143 yr^{-1}), the excess Q_{ss} attributable to the earthquake was $14.3 \pm 7.8 \text{ Mt yr}^{-1}$ (Table DR1). Most
144 (>95%) of this mass is fine sediment, <0.25 mm (Fig. DR4). In contrast, $2.4+1.9/-0.7 \text{ km}^3$ of
145 sediment was mobilized by earthquake-triggered landslides (Li et al., 2014), equating to
146 $6329+5097/-1787 \text{ Mt}$ (assuming a solid density of $2.65 \times 10^3 \text{ kg m}^{-3}$). Of this sediment, available
147 data suggests that $6.6 \pm 4.4\%$ has a grain size of <0.25 mm (Table DR3). Acknowledging the
148 uncertainty on these estimates, we estimate a total supply of fine (<0.25 mm) landslide sediment of
149 $418+437/-302 \text{ Mt}$.

150 Across the Longmen Shan, at the present rate of post-earthquake fluvial export, we
151 estimate that it will take $29+30/-21$ years to remove all material <0.25 mm delivered by coseismic
152 landslides (Table DR1). This estimate does not consider a decline in Q_{ss} over time (Fig. 2C) and so
153 provides a lower bound on residence time. Estimates of fine sediment residence time in individual
154 catchments range from $1.0+1.6/-0.9$ to $77+109/-65 \text{ yr}$, with an extreme value of $190+528/-186 \text{ yr}$
155 (Table DR1). The residence time estimated from Fujiangqiao station ($5+8/-4 \text{ yr}$) is consistent with
156 the estimate made from the decline of sediment load in this catchment of $6 \pm 1 \text{ yr}$ (Fig. 2C).

157 **CONTROLS ON SEDIMENT RESIDENCE TIME**

158 The estimated residence times of fine-grained coseismic landslide sediment in the
159 Longmen Shan span the range estimated from previous earthquakes (Pain and Bowler, 1973;

160 Pearce and Watson, 1986; Koi et al., 2008, Hovius et al., 2011; Howarth et al., 2012). Here we
161 assess the controls on this variability. For a given catchment hydrological regime and transport
162 capacity, an increase in sediment supply should increase the residence time of that sediment
163 (Pearce and Watson, 1986; Benda and Dunne, 1997; Yanites et al., 2010). The data from the
164 Longmen Shan are broadly consistent with this hypothesis: catchments with low coseismic
165 landslide density ($\rho_{ls} < 0.2\%$) generally have shorter fine sediment residence times than those with
166 $\rho_{ls} > 0.6\%$ (Fig. 3), assuming that V_{ls} scales with A_{ls} . However, this only partly explains the
167 variability between catchments.

168 In the Longmen Shan, the contribution of intense runoff events (daily Q_w normalized by
169 catchment area) varies between catchments (Fig. DR5). The proportion of total catchment runoff
170 delivered by daily flows $>5 \text{ mm day}^{-1}$ varies from 0 to 66% across the study area (Table DR1). For
171 a given landslide density, a higher proportion of intense runoff leads to a shorter fine sediment
172 residence time (Fig. 3), likely due to a combination of increased river transport capacity and
173 enhanced mobilization of sediment from existing deposits (Benda and Dunne, 1997; Dadson et al.,
174 2004). In addition, heavy rainfall can trigger landslides on earthquake-weakened slopes (Dadson
175 et al., 2004). The very long fine residence time in Santai ($187+510/-153 \text{ yr}$) is more than double
176 any other catchment and cannot be well explained by runoff intensity and ρ_{ls} alone. There, the very
177 long residence time may reflect large individual landslides that contribute significant volumes of
178 sediment but limited total landslide area (Fig. DR6). The additional variability (Fig. 3) may be due
179 to secondary factors (e.g. spatial variability in landslide connectivity, channel order, channel

180 gradients, channel length, and anthropogenic activities) which can moderate Q_{ss} (Benda and
181 Dunne, 1997). The scatter also reflects the uncertainty in the quantification of residence time,
182 derived mainly from uncertainty in the volume of fine sediment from landslides and its grain size.
183 Nevertheless, our data suggest that runoff intensity plays a crucial role in regulating the residence
184 time of fine sediment mobilized by a major earthquake (Fig. 3).

185 **WIDER IMPLICATIONS**

186 Our analysis can explain the relatively short residence time of fine sediment after the 1999
187 M_w 7.6 Chi-Chi earthquake in Taiwan (Hovius et al., 2011) as compared with the range of
188 responses in the Longmen Shan catchments (Fig. 3). In Taiwan, 11 large tropical cyclones in
189 1999-2007 each delivered the annual runoff of the Longmen Shan ($\sim 0.4\text{--}0.7$ m, $\sim 1\text{--}2$ km³ of
190 water) over a period of 10–30 days (Hovius et al., 2011). This intense runoff delivery is reflected in
191 the Chenyoulan catchment, where $\sim 60\%$ of the annual runoff is delivered by events with >5 mm
192 day⁻¹, higher than any catchment impacted by Wenchuan earthquake (Figs. 3 and DR5). These
193 cyclones triggered additional post-seismic landslides (Dadson et al., 2004). Despite this additional
194 sediment input, suspended sediment loads returned to pre-earthquake levels in ~ 6 yr. The
195 short-lived fluvial influence of Chi-Chi landslide sediment can thus be attributed to intense
196 precipitation during tropical cyclones, which enables the rapid erosion, transport and export of
197 landslide-mobilized sediment. These observations are also consistent with lake records of fine
198 sediment accumulation driven by earthquakes on the Alpine Fault, New Zealand. There, enhanced
199 sediment export from catchments appears to last for ~ 50 yr following earthquakes (Howarth et al.,

200 2012). While total runoff is high in the western Southern Alps, it is delivered at a lower intensity
201 than in Taiwan (Dadson et al., 2004; Hovius et al., 2011).

202 Our results suggest that the combination of coseismic landslide density and the frequency
203 of intense runoff events appears to govern, to first order, the residence time of fine-grained
204 sediment (Fig. 3). This may also be the case for coarser sediment, but it is not straightforward to
205 extend our analysis to coarse-grained landslide material transported as bed load (Pearce and
206 Watson, 1986; Korup et al., 2004) which can reside in catchments for much longer periods of time
207 (Benda and Dunne, 1997; Yanites et al., 2010; Huang and Montgomery, 2012). Nevertheless, river
208 catchments with high coseismic landslide density and infrequent high runoff events may have long
209 memories of large earthquakes (Fig. 3), posing a significant challenge to hazard management
210 (Huang and Fan, 2013).

211 **ACKNOWLEDGMENTS**

212 This research was funded by the 973 program (2013CB956402) to Z.J., NSFC grants
213 and CAS YIS Fellowships to A.J.W. and R.G.H., a U.S. NSF Grant (EAR/GLD 1053504) to
214 A.J.W., and a Royal Society Grant (RG110569) to R.G.H. We thank Y. Peng, F. Li, and Q.
215 Zhang for assistance in the data collection and A. Galy, P. Molnar, R. Parker and J. Yu for
216 discussions during manuscript preparation. J. Spotila, D. Lague, I. Larsen and three
217 anonymous referees are thanked for their insightful comments which improved the manuscript.

218 **REFERENCES CITED**

- 219 Benda, L., and Dunne, T., 1997, Stochastic forcing of sediment supply to channel networks from
220 landsliding and debris flow: *Water Resources Research*, v. 33, p. 2849–2863,
221 doi:10.1029/97WR02388.
- 222 Dadson, S.J., Hovius, N., Chen, H., Dade, W.B., Lin, J.-C., Hsu, M.-L., Lin, C.-W., Horng, M.-J.,
223 Chen, T.-C., Milliman, J., and Stark, C.P., 2004, Earthquake-triggered increase in sediment
224 delivery from an active mountain belt: *Geology*, v. 32, p. 733–736, doi:10.1130/G20639.1.
- 225 Glade, T., and Crozier, M.J., 2005, The nature of landslide hazard impact, *in* Glade, T., Anderson,
226 M., and Crozier, M.J., eds., *Landslide Hazard and Risk*: Chichester, John Wiley & Sons, Ltd,
227 p. 41–74.
- 228 Guzzetti, F., Ardizzone, F., Cardinali, M., Rossi, M., and Valigi, D., 2009, Landslide volumes and
229 landslide mobilization rates in Umbria, central Italy: *Earth and Planetary Science Letters*,
230 v. 279, p. 222–229, doi:10.1016/j.epsl.2009.01.005.
- 231 Hovius, N., Meunier, P., Lin, C.-W., Chen, H., Chen, Y.-G., Dadson, S., Horng, M.-J., and Lines,
232 M., 2011, Prolonged seismically induced erosion and the mass balance of a large earthquake:
233 *Earth and Planetary Science Letters*, v. 304, p. 347–355, doi:10.1016/j.epsl.2011.02.005.
- 234 Howarth, J.D., Fitzsimons, S.J., Norris, R.J., and Jacobsen, G.E., 2012, Lake sediments record
235 cycles of sediment flux driven by large earthquakes on the Alpine fault, New Zealand:
236 *Geology*, v. 40, p. 1091–1094, doi:10.1130/G33486.1.

- 237 Huang, M.Y.-F., and Montgomery, D.R., 2012, Fluvial response to rapid episodic erosion by
238 earthquake and typhoons, Tachia River, central Taiwan: *Geomorphology*, v. 175–176, p.
239 126–138, doi:10.1016/j.geomorph.2012.07.004.
- 240 Huang, R., and Fan, X., 2013, The landslide story: *Nature Geoscience*, v. 6, p. 325–326,
241 doi:10.1038/ngeo1806.
- 242 Keefer, D.K., 1984, Landslides caused by earthquakes: *Geological Society of America Bulletin*,
243 v. 95, p. 406–421, doi:10.1130/0016-7606(1984)95<406:LCBE>2.0.CO;2.
- 244 Keefer, D.K., 1994, The importance of earthquake-induced landslides to long-term slope erosion
245 and slope-failure hazards in seismically active regions: *Geomorphology*, v. 10, p. 265–284,
246 doi:10.1016/0169-555X(94)90021-3.
- 247 Koi, T., Hotta, N., Ishigaki, I., Matuzaki, N., Uchiyama, Y., and Suzuki, M., 2008, Prolonged
248 impact of earthquake-induced landslides on sediment yield in a mountain watershed: The
249 Tanzawa region, Japan: *Geomorphology*, v. 101, p. 692–702,
250 doi:10.1016/j.geomorph.2008.03.007.
- 251 Korup, O., McSaveney, M.J., and Davies, T.R.H., 2004, Sediment generation and delivery from
252 large historic landslides in the Southern Alps, New Zealand: *Geomorphology*, v. 61, p. 189–
253 207, doi:10.1016/j.geomorph.2004.01.001.
- 254 Larsen, I.J., Montgomery, D.R., and Korup, O., 2010, Landslide erosion controlled by hillslope
255 material: *Nature Geoscience*, v. 3, p. 247–251, doi:10.1038/ngeo776.

- 256 Li, G., West, A.J., Densmore, A.L., Jin, Z., Parker, R.N., and Hilton, R.G., 2014, Seismic
257 mountain building: Landslides associated with the 2008 Wenchuan earthquake in the context
258 of a generalized model for earthquake volume balance: *Geochemistry Geophysics*
259 *Geosystems*, v. 15, p. 833–844, doi:10.1002/2013GC005067.
- 260 Liu-Zeng, J., Wen, L., Oskin, M., and Zeng, L., 2011, Focused modern denudation of the
261 Longmen Shan margin, eastern Tibetan Plateau: *Geochemistry Geophysics Geosystems*,
262 v. 12, Q11007, doi:10.1029/2011GC003652.
- 263 Ministry of Water Resources of China, 2007, Code for Measurements of Suspended Sediment in
264 Open Channels (GB50159–92): Beijing, China Planning Press (in Chinese).
- 265 Pain, C., and Bowler, J., 1973, Denudation following the November 1970 earthquake at Madang,
266 Papua New Guinea: *Zeitschrift fur Geomorphologie*, v. 18, supplement, p. 92–104.
- 267 Parker, R.N., Densmore, A.L., Rosser, N.J., de Michele, M., Li, Y., Huang, R., Whadcoat, S., and
268 Petley, D.N., 2011, Mass wasting triggered by the 2008 Wenchuan earthquake is greater than
269 orogenic growth: *Nature Geoscience*, v. 4, p. 449–452, doi:10.1038/ngeo1154.
- 270 Pearce, A.J., and Watson, A.J., 1986, Effects of earthquake-induced landslides on sediment budget
271 and transport over a 50-yr period: *Geology*, v. 14, p. 52–55,
272 doi:10.1130/0091-7613(1986)14<52:EOELOS>2.0.CO;2.
- 273 USGS, U.S. Geological Survey Earthquake Hazards Program:
274 <http://earthquake.usgs.gov/earthquakes/map/>, (accessed August 2013).

275 West, A.J., Hetzel, R., Li, G., Jin, Z., Zhang, F., Hilton, R.G., and Densmore, A.L., 2014, Dilution
276 of Be-10 in detrital quartz by earthquake-induced landslides: Implications for determining
277 denudation rates and potential to provide insights into landslide sediment dynamics: Earth and
278 Planetary Science Letters, v. 396, p. 143–153, doi:10.1016/j.epsl.2014.03.058.

279 Xu, X., Wen, X., Yu, G., Chen, G., Klinger, Y., Hubbard, J., and Shaw, J., 2009, Coseismic
280 reverse- and oblique-slip surface faulting generated by the 2008 Mw 7.9 Wenchuan
281 earthquake, China: Geology, v. 37, p. 515–518, doi:10.1130/G25462A.1.

282 Yanites, B.J., Tucker, G.E., Mueller, K.J., and Chen, Y.G., 2010, How rivers react to large
283 earthquakes: Evidence from central Taiwan: Geology, v. 38, p. 639–642,
284 doi:10.1130/G30883.1.

285 **FIGURE CAPTIONS**

286 Figure 1. Major rivers impacted by the 2008 M_w 7.9 Wenchuan earthquake in the Longmen Shan,
287 China (Min Jiang, Fu Jiang, and Tuo Jiang). River gauging stations used in this study are shown as
288 circles. Nested gauging stations shown in Figure 2B and 2C are highlighted in yellow. Catchment
289 color reflects the ratio of mean annual suspended sediment discharge (Q_{ss} , Mt yr⁻¹) after the
290 earthquake to that prior to the earthquake. Contours show landslide areal density ρ_{ls} (%) calculated
291 as the proportion of total area mapped as landslides (Li et al., 2014). Columns show the
292 background Q_{ss} (white) and post-earthquake Q_{ss} (red).

293 Figure 2. Fluvial response to the 2008 Wenchuan earthquake. **A.** Suspended sediment
294 concentration (SSC) measurements from the Zagunao River (Sangping station) in May 2008

295 before (gray circles) and after (red circles) the earthquake (red dashed line) and those taken shortly
296 after aftershocks (blue dashed lines) within ~20 km of the gauging station (blue circles). Solid red
297 line ($r^2 = 0.51$) is linear least-square best fit to the SSC data from 13 to 22 May. Daily water
298 discharge normalized to the 2006-2011 average (Q_w/Q_{mean}) is shown as thicker solid line (gray). **B.**
299 Downstream sediment gain on the Zagunao River – the ratio of downstream (Sangping station) to
300 upstream (Zagunao station) Q_{ss} (Fig. 1). **C.** Downstream sediment gain on the Fu Jiang – the ratio
301 of downstream (Fujiangqiao) to upstream (Pingwu) Q_{ss} . The dashed line is the best-fit power-law
302 fit with 95% confidence intervals shown by dotted lines. On all panels whiskers show uncertainties
303 (1σ) if larger than the point size.

304 Figure 3. Estimates of fine (<0.25 mm) coseismic landslide sediment residence time in river
305 catchments impacted by the Wenchuan earthquake (circles), plotted as a function of the proportion
306 of catchment runoff delivered by intense flows (> 5 mm day⁻¹) from May 2008 to Dec 2012.
307 Shading of points reflects the upstream landslide areal density (%). Whiskers show propagated
308 uncertainties of residence time of fine grained sediment. Star indicates comparable estimate from
309 the 1999 Chi-Chi earthquake, Taiwan (Hovius et al., 2011).

310 ¹GSA Data Repository item 2014xxx, Figures DR1-6, Tables DR1-3 and Supplementary
311 Information, is available online at www.geosociety.org/pubs/ft2014.htm, or on request from
312 editing@geosociety.org or Documents Secretary, GSA, P.O. Box 9140, Boulder, CO 80301, USA.

Figure 1

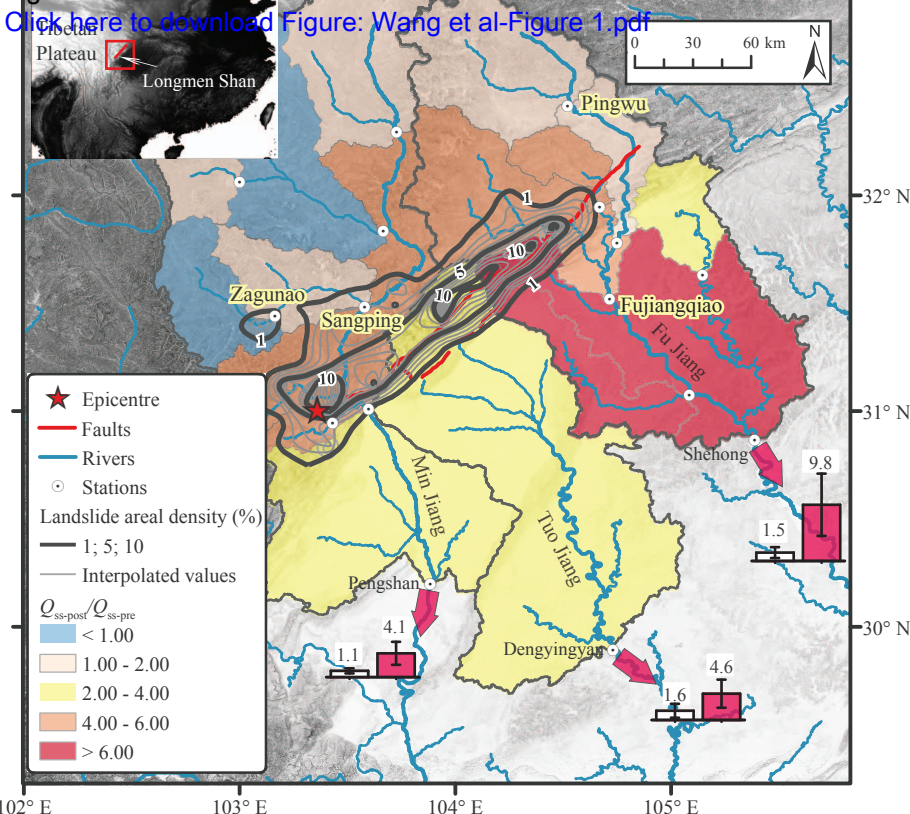


Figure 2

[Click here to download Figure: Wang et al-Figure 2.pdf](#)

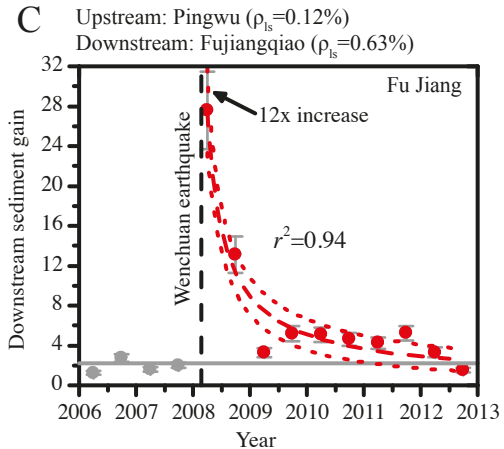
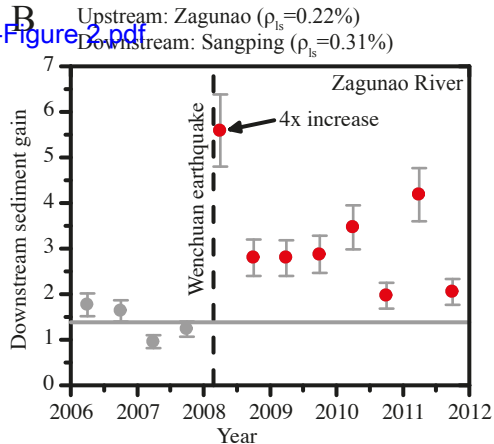
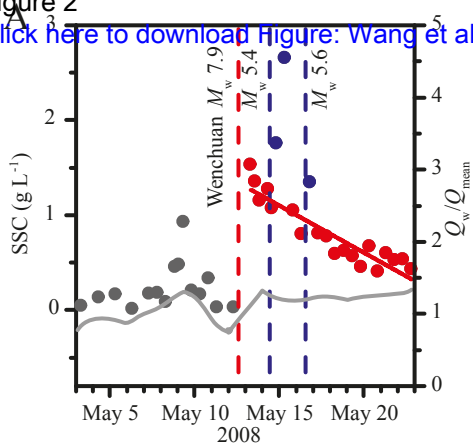
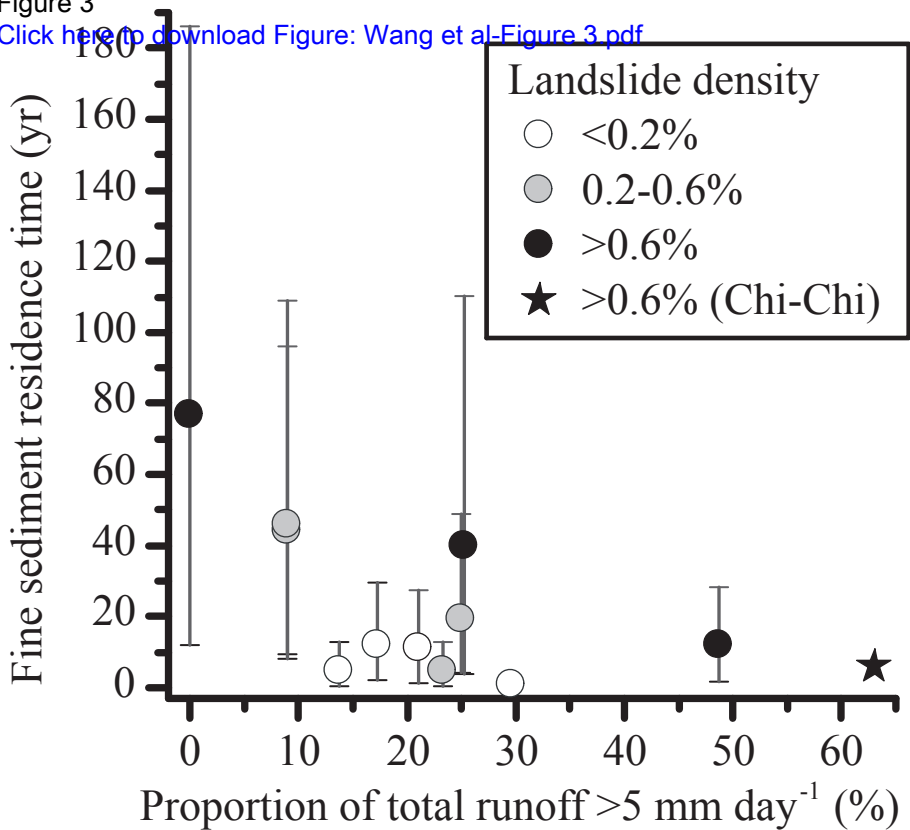


Figure 3

[Click here to download Figure: Wang et al-Figure 3.pdf](#)



1 GSA DATA REPOSITORY

2 Controls on fluvial evacuation of sediment from
3 earthquake-triggered landslides

4 **Jin Wang^{1,2,3}, Zhangdong Jin^{1,4*}, Robert G. Hilton², Fei Zhang¹, Alexander L.
5 Densmore^{2,5}, Gen Li⁶, and A. Joshua West⁶**

6 ¹ *State Key Laboratory of Loess and Quaternary Geology, Institute of Earth
7 Environment, Chinese Academy of Sciences, Xi'an 710075, China*

8 ² *Department of Geography, Durham University, Durham, DH1 3LE, UK*

9 ³ *University of Chinese Academy of Sciences, Beijing 100049, China*

10 ⁴ *Institute of Global Environmental Change, Xi'an Jiaotong University, Xi'an 710049,
11 China*

12 ⁵ *Institute of Hazard, Risk and Resilience, Durham University, Durham, DH1 3LE,
13 UK*

14 ⁶ *Department of Earth Sciences, University of Southern California, Los Angeles, CA
15 90089, USA*

16

17

18

19

20

21

22

23 **Grain Size Distribution of Landslide Deposits**

24 In this study, we use published measurements of the grain size distribution of
25 landslide deposits formed during the 2008 Wenchuan earthquake (Table DR3) (Wang
26 et al., 2011; Chen et al., 2012; Wang et al., 2012; Zhuang et al., 2012; Wang et al.,
27 2013; Yu et al., 2013). Full details of methods can be found in these publications.
28 Here, for summary, the procedure described by Wang et al. (2013) is provided. The
29 grain size distribution of landslide sediment was analyzed by sieving and photography
30 at 11 locations on the Tianchi landslide dam deposit. The area ratio of large grains
31 with $\phi > 40$ mm was measured by means of particle digital image analysis, using
32 vertical photographs that were taken from a height of approximately 1.5 m above the
33 ground surface. All visible individual grains > 4.75 mm were outlined on the
34 photographs, with the intermediate (b-axis) diameter and the cross-sectional area
35 determined for each grain. For grains < 4.75 mm, a 10 kg sample of ≤ 50 mm sediment
36 was collected from each site and was sieved upon return to the laboratory. ASTM
37 standards sieve series were utilized for this task. Assuming that the sediment has the
38 same density, the weight percentages of grains with different grain sizes were
39 calculated.

40 **Grain Size Distribution of Suspended Sediments**

41 The grain size distributions of suspended sediments were determined from samples
42 collected from the three main rivers in the study area on the Min Jiang
43 (Zhenjianguan station), Tuo Jiang (Dengyingyan station) and Fu Jiang (Fujiangqiao
44 station) (Fig. 1). The analyses were undertaken by the methods described in detail by

45 Guy (1969) and the Ministry of Water Resources of China (2005) and a summary is
46 provided here. A depth-integrated and channel averaged suspended sediment sample
47 was collected. Calgon solution was added to disperse and disaggregate clay particles
48 and the sample was sieved at 0.063 mm. The >0.063 mm fraction was oven-dried at
49 100°C and the grain size distribution was determined by dry sieving at 2 mm, 1 mm,
50 0.5 mm, 0.25 mm and 0.125 mm. The <0.063 mm fraction was transferred to a 1 L
51 graduated cylinder and was mixed for one minute until homogenized. Immediately
52 after, 25 mL water was pipetted from the middle of cylinder to determine the total
53 suspended load. Based on the predictable relationship between particle grain size and
54 settling velocity in a fluid medium, the time and depth of subsequent pipette aliquots
55 was determined on the basis of the Stokes law (e.g. for 25°C, time = 1'43", D = 0.031
56 mm; time = 6'26", D = 0.016 mm; time = 25'45", D = 0.008 mm; time = 1h 43', D =
57 0.004 mm). The pipetted samples were dried and weighed.

58 Table DR1. Landslide input and suspended sediment discharge of sixteen gauging stations along the Longmen Shan.

Station	River	Area (km ²)	Runoff (mm yr ⁻¹)	Proportion >5 mm day ⁻¹ (%)	Q_{ss-pre} (Mt yr ⁻¹)	$Q_{ss-post}$ (Mt yr ⁻¹)	Landslide area (km ²)	Landslide density (%)	Landslide input (Mt)	M_{fines} (Mt)	T_{fines} (yr)
Zhenjiangguan	Min J.	4,486	350±76	1.3	0.46±0.05	0.64±0.06	*	*	*	*	-
Heishui	Min J.	1,720	773±84	21.0	0.30±0.03	0.30±0.03	0.05	< 0.01	0.5+0.7/-0.3	0.03+0.05/-0.03	11+16/-10
Shaba	Min J.	7,231	543±81	5.4	1.55±0.16	0.77±0.08	0.23	< 0.01	2.1+2.0/-0.9	0.14+0.16/-0.11	-
Zagunao	Min J.	2,404	808±83	17.5	0.65±0.07	0.53±0.05	5.53	0.22	69+97/-40	5+7/-4	-
Sangping	Min J.	4,629	673±74	8.9	0.83±0.08	1.06±0.11	12.3	0.27	153+150/-63	10+12/-8	44+52/-34
Guojiaba	Min J.	555	663±184	48.7	0.10±0.01	0.57±0.06	9.71	1.71	84+101/-46	5+8/-5	12+16/-10
Dujiang	Min J.	22,947	349±32	0	0.39±0.04	2.12±0.21	163	0.71	2018+2529/-1039	133+189/-112	77+109/-65
Pingwu	Fu J.	4,310	764±121	13.7	1.38±0.14	2.60±0.26	5.02	0.12	85+147/-53	6+10/-5	5+9/-4
Jiangyou	Fu J.	5,915	515±93	17.2	1.59±0.16	2.27±0.23	8.37	0.14	125+158/-58	8+12/-7	12+17/-10
Ganxi	Fu J.	1,067	509±102	29.6	0.28±0.03	1.36±0.14	1.44	0.14	17+23/-10	1.1+1.7/-1.0	1.0+1.6/-0.9
Fujiangqiao	Fu J.	11,903	644±105	23.3	3.10±0.31	14.50±1.45	52.5	0.45	800+1282/-486	53+92/-48	5+8/-4
Zitong	Fu J.	1,547	512±196	66.0	0.27±0.03	0.73±0.07	*	*	*	*	-
Santai	Fu J.	2,343	442±114	33.2	0.07±0.01	0.47±0.05	20.2	0.79	1131+3056/-816	75+208/-73	190+528/-186
Pengshan	Min J.	30,661	372±82	8.9	1.09±0.11	4.14±0.41	172	0.56	2125+2534/-1040	140+192/-116	46+63/-38
Dengyingyan	Tuo J.	14,484	583±113	25.3	1.61±0.16	4.58±0.46	109	0.74	1789+2933/-1096	118+209/-107	40+70/-36
Shehong	Fu J.	23,574	480±87	25.0	1.46±0.15	9.78±0.98	109	0.47	2415+3386/-991	159+247/-125	19+30/-15
Total	-	68,719	478±126	-	4.56±0.46	18.50±1.85	390	0.57	6329+5097/-1787	418+437/-302	29+30/-21

59 *Negligible landslide coverage.

60 The runoff is based on the time period of 2006-2012 except Sangping station (2006-2011). Q_{ss-pre} and $Q_{ss-post}$ are the average annual suspended sediment discharges before (2006-2007) and after (2008-2012) the
61 earthquake, respectively. M_{fines} (Mt) is the estimated mass of landslide material with a grain size < 0.25 mm, which accounts for 4-9% of the total landslide mass. T_{fines} (yr) is the estimated time necessary for rivers to
62 remove all M_{fines} based on the post-earthquake removal rates.

63 Table DR2. Uncertainty of suspended-sediment discharge at the Sangping station.

Year	<i>n</i>	Standard Deviation (%)	Standard Error (%)
2006	113	12.6	5.1
2007	112	12.3	5.8
2008	158	6.1	3.3
2009	117	8.1	4.6
total	500	10.1	4.9

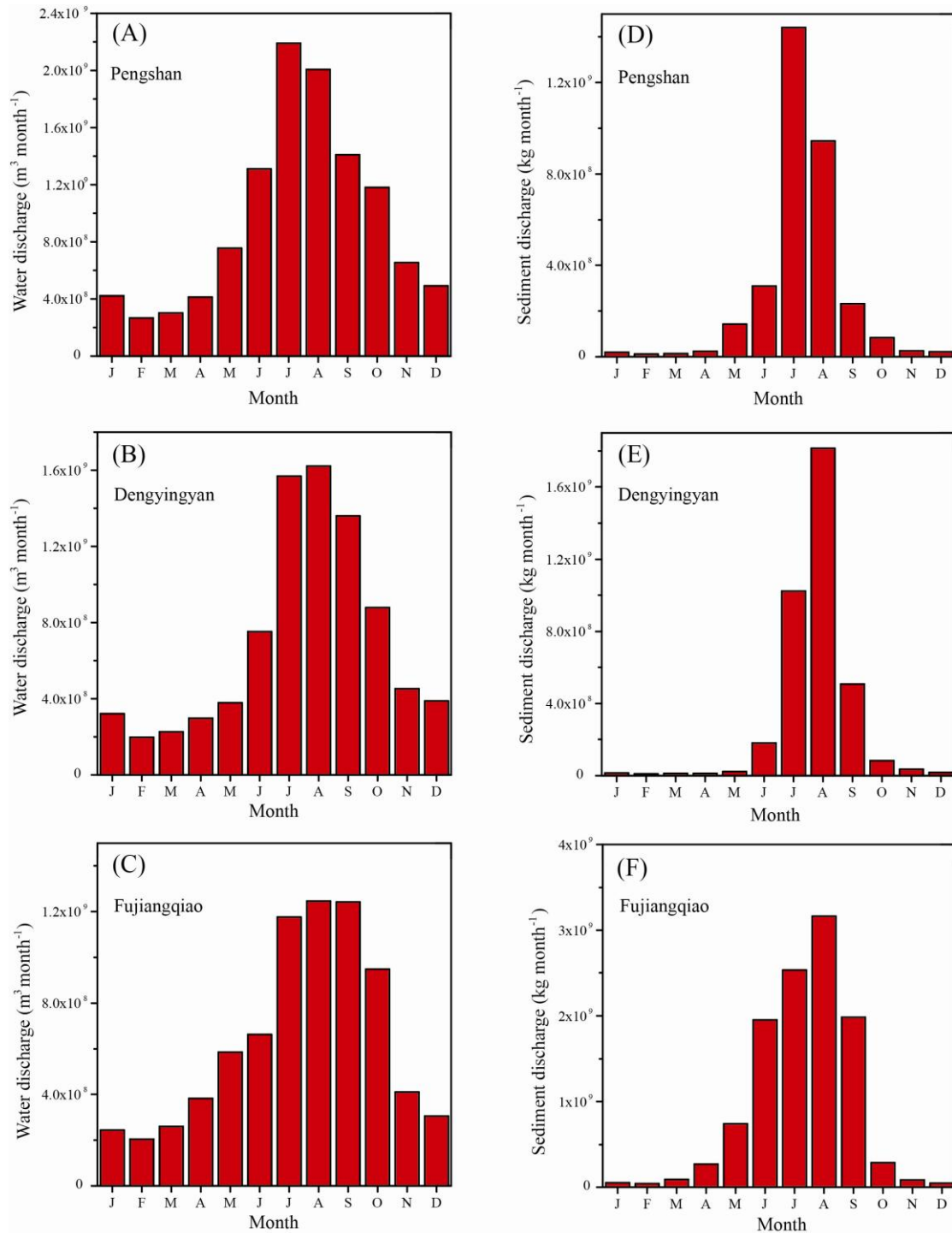
64 *n* is the number of days with more than one SSC measurement. The standard deviation and
 65 standard error are reported as a percentage of the mean SSC.

66
 67
 68
 69
 70
 71
 72
 73
 74
 75
 76
 77
 78
 79
 80
 81
 82
 83
 84
 85
 86
 87
 88
 89
 90
 91
 92
 93
 94
 95
 96
 97
 98
 99
 100

101 Table DR3. Proportion of grains <0.25 mm from deposits of landslides triggered by the Wenchuan
 102 earthquake.

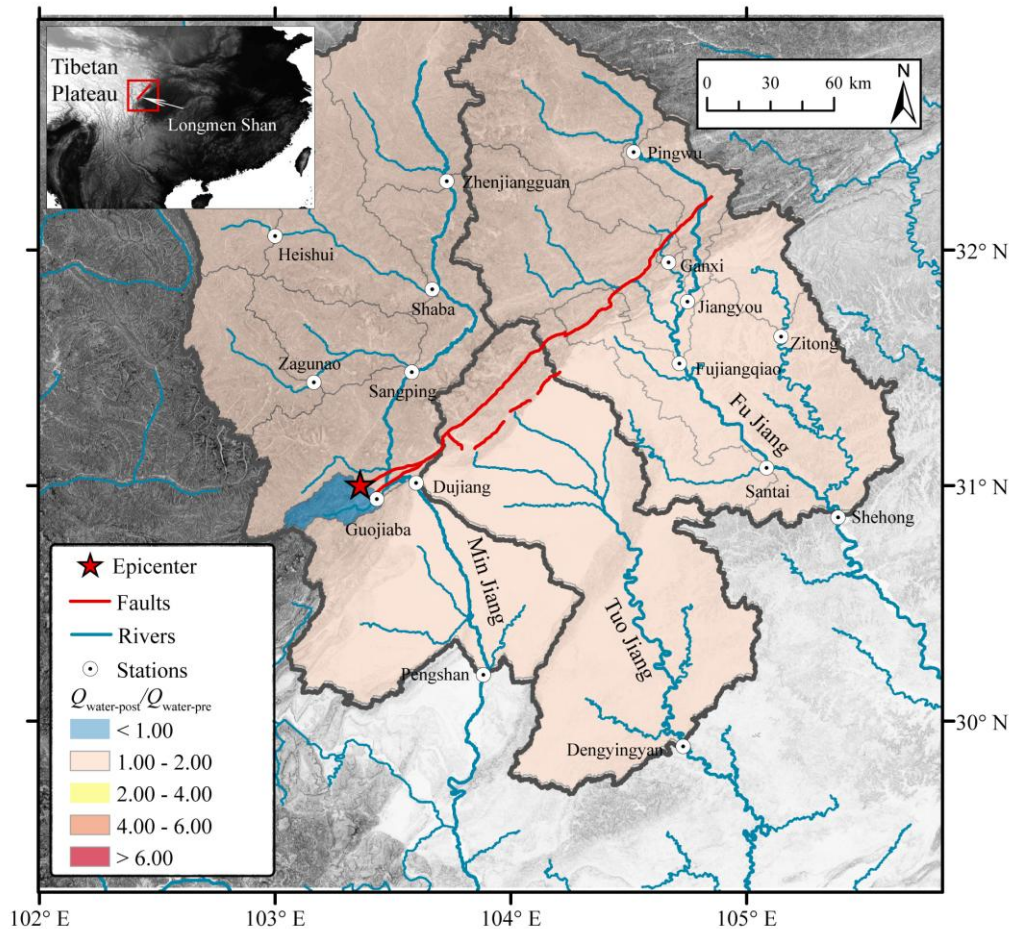
Site	Catchment	Weight % <0.25 mm	Reference
Xiaojiagou, Yingxiu S1	Min Jiang	3.0%	1
Xiaojiagou, Yingxiu S2	Min Jiang	6.0%	1
Xiaojiagou, Yingxiu S3	Min Jiang	3.0%	1
Xiaojiagou, Yingxiu S4	Min Jiang	3.0%	1
Xiaojiagou, Yingxiu S5	Min Jiang	3.0%	1
Xiaojiagou, Yingxiu S6	Min Jiang	3.0%	1
Xiaojiagou, Yingxiu S7	Min Jiang	3.0%	1
Xiaojiagou, Yingxiu S8	Min Jiang	5.0%	1
Niuquangou - a	Min Jiang	8.2%	2
Niuquangou - b	Min Jiang	7.0%	2
Niuquangou - c	Min Jiang	10.3%	2
Xiejiadianzi - a	Tuo Jiang	6.4%	2
Xiejiadianzi - b	Tuo Jiang	5.1%	2
Xiejiadianzi - c	Tuo Jiang	6.0%	2
Xiejiadianzi - d	Tuo Jiang	1.2%	2
Wenjiagou - a	Tuo Jiang	5.3%	2
Wenjiagou - b	Tuo Jiang	2.8%	2
Wenjiagou - c	Tuo Jiang	8.8%	2
Wenjiagou - d	Tuo Jiang	2.6%	2
Mianyuan River, p6	Tuo Jiang	3.8%	3
Mianyuan River, p9	Tuo Jiang	5.2%	3
Mianyuan River, p7	Tuo Jiang	7.4%	3
Mianyuan River, p11	Tuo Jiang	9.6%	3
Mianyuan River, p5	Tuo Jiang	10.8%	3
Mianyuan River, p10	Tuo Jiang	13.4%	3
Wenjiagou, site 1	Tuo Jiang	2.0%	4
Wenjiagou, site 2	Tuo Jiang	22.9%	4
Shiting River	Tuo Jiang	6.1%	5
Qingzhu River	Fu Jiang	4.3%	5
Weijiagou, site 1	Fu Jiang	6.1%	6
Weijiagou, site 2	Fu Jiang	6.7%	6
Weijiagou, site 3	Fu Jiang	8.7%	6
Weijiagou, site 4	Fu Jiang	16.8%	6
Average (n=33)		6.6±4.4%	

103 References: 1, Chen et al., 2012; 2, Wang et al., 2012; 3, Wang et al., 2013; 4, Yu et al., 2013; 5,
 104 Wang et al., 2011; 6, Zhuang et al., 2012.



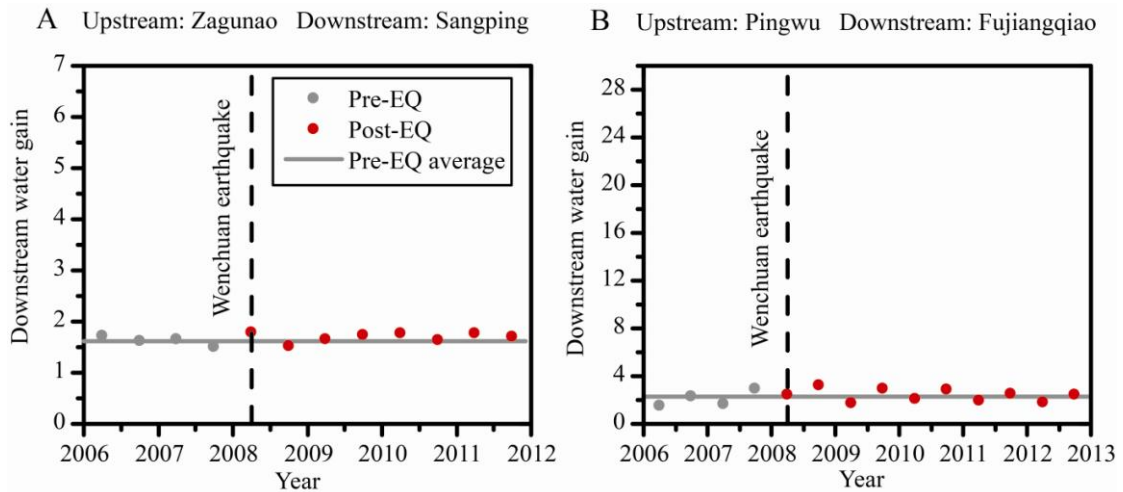
105

106 **Figure DR1: Monthly variations of water discharge ($\text{m}^3 \text{ month}^{-1}$) and suspended**
 107 **sediment discharge (kg month^{-1}) at three typical stations across the Longmen**
 108 **Shan from 2006 to 2012. (A and D) Pengshan station, (B and E) Dengyingyan station,**
 109 **and (C and F) Fujiangqiao station. Water discharge during April to October accounts**
 110 **for ~81% of total annual discharge, whereas suspended sediment discharge accounts**
 111 **for ~97% at these stations.**



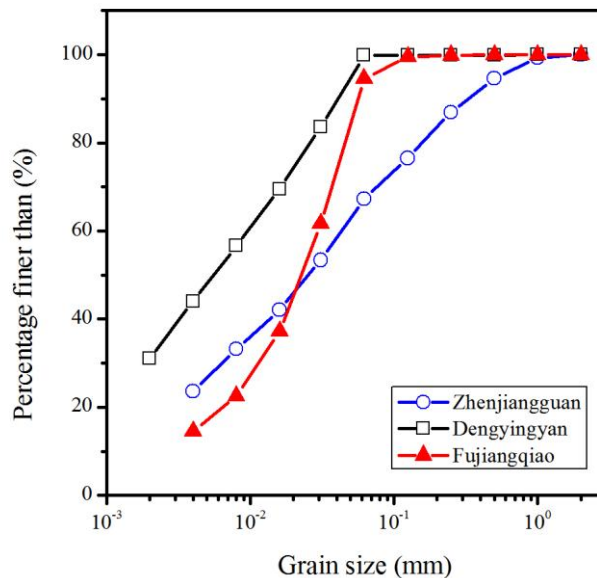
112
 113
 114
 115
 116
 117
 118
 119
 120
 121

Figure DR2: Water discharge enhancement in rivers of the Longmen Shan following the Wenchuan earthquake. Catchment shadings reflect the ratios of mean annual water discharge (Q_{water} , $\text{m}^3 \text{yr}^{-1}$) after the Wenchuan earthquake to that prior to the earthquake for available gauging stations (circles). In order to compare with the ratios of suspended sediment enhancement in Fig. 1, we use the same class ranges for colour shadings. The large discrepancy between the water discharge enhancement (shown here) and the suspended sediment enhancement (Fig. 1) demonstrates that the changes of sediment load are not caused by variation in water discharge.



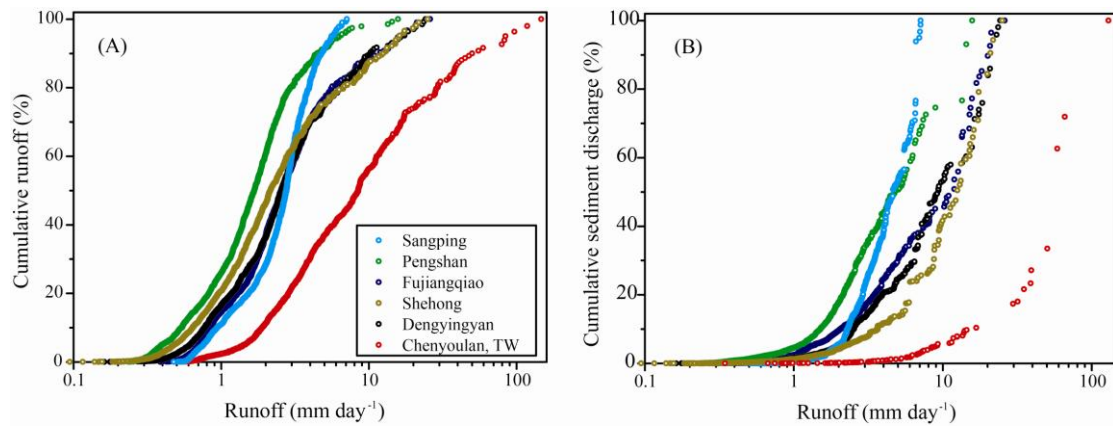
122
123
124
125
126
127
128

Figure DR3: A. Downstream water gain for nested gauging stations on the Zagunao River. B. Downstream water gain for nested gauging stations on the Fu Jiang. Downstream water gain is the ratio of downstream to upstream water discharge. In order to compare with the downstream sediment gain in Fig. 2B and 2C, we use the same ranges of axes.



129
130
131
132
133
134
135
136
137
138

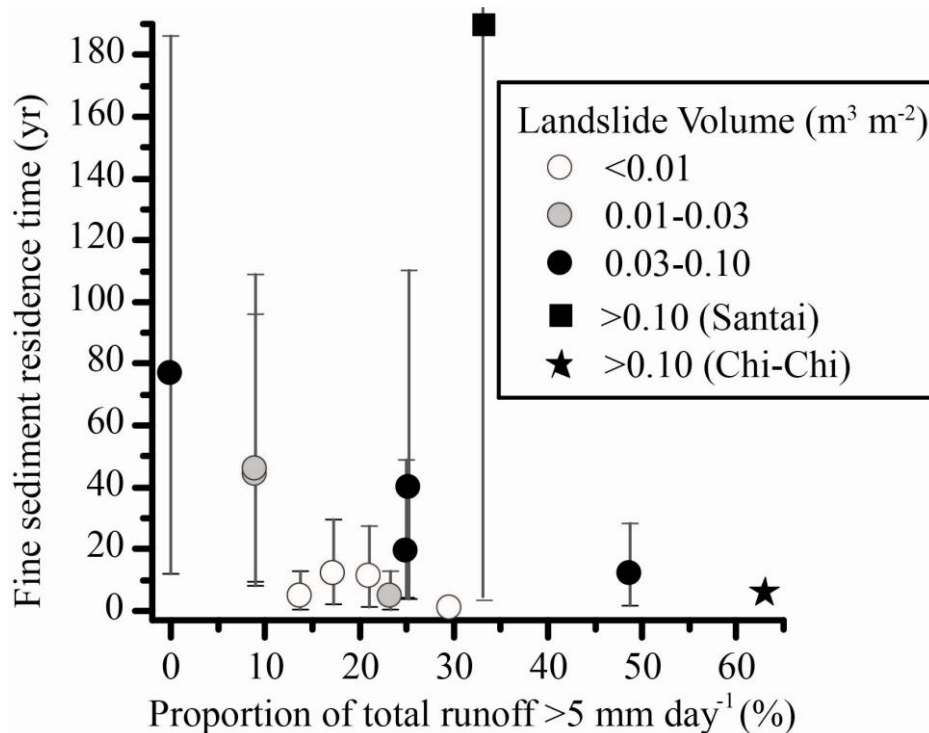
Figure DR4: Grain size distribution of suspended sediment in our studied rivers during 2007 to 2012. Over 95% of suspended sediment grain size is smaller than 0.25 mm. The blue line with open circles is grain size distribution of suspended sediment collected from Zhenjiangguan station on the Min Jiang; black line with squares is from Dengyingyan station on the Tuo Jiang; and the red line with triangles is from Fujiangqiao station on the Fu Jiang. The method for determining the grain size distribution followed the standard of the Ministry of Water Resources of China (2005).



139

140 **Figure DR5: The cumulative runoff (A) and sediment discharge (B) in Longmen**
 141 **Shan and in the Chenyoulan River, Taiwan after the Wenchuan and Chi-Chi**
 142 **earthquakes.** Comparing to the rivers in the Longmen Shan, the Chenyoulan River
 143 has higher runoff, with higher frequency of high runoff events. Most of suspended
 144 sediment is mobilized during high runoff events.

145



146

147 **Figure DR6: Estimates of residence time of fine grained sediment mobilized by**
 148 **earthquake-triggered landslides in river catchments impacted by Wenchuan**
 149 **earthquake, plotted as a function of proportion of catchment intense runoff (>5**
 150 **mm day⁻¹).** Compared to Fig. 3, the symbols reflect the landslide volume per unit area
 151 caused by coseismic landslide. The residence time of Santai station (square, landslide
 152 density = 0.79%) is not well explained by the control of landslide density in Fig. 3.
 153 This is because there are some individual landslides with large volume, which
 154 contribute significant volumes of sediment, but this is not reflected in landslide area in
 155 this small (2,300 km²) catchment.

- 156 References cited:
157 Chen, H.X., Zhang, L.M., Chang, D.S., and Zhang, S., 2012, Mechanisms and runout characteristics of
158 the rainfall-triggered debris flow in Xiaojiagou in Sichuan Province, China: *Natural Hazards*,
159 v. 62, p. 1037-1057, doi: 10.1007/s11069-012-0133-5.
160 Guy, H.P., 1969, Laboratory theory and methods for sediment analysis: U.S. Geological Survey
161 Techniques of Water Resources Investigations, book 5, chap. C1, p. 23-28.
162 Ministry of Water Resources of China, 2005, Technical Standard for Determination of Sediment
163 Particle Size in Open Channels (SL 42–2010): Beijing, China Water and Power Press (in
164 Chinese).
165 Wang, G., Huang, R., Kamai, T., and Zhang, F., 2013, The internal structure of a rockslide dam induced
166 by the 2008 Wenchuan ($M_w7.9$) earthquake, China: *Engineering Geology*, v. 156, p. 28-36, doi:
167 10.1016/j.enggeo.2013.01.004.
168 Wang, Y., Cheng, Q., and Zhu, Q., 2012, Inverse grading analysis of deposit from rock avalanches
169 triggered by wenchuan earthquake: *Chinese Journal of Rock Mechanics and Engineering*, v.
170 31, p. 1089-1106 (in Chinese).
171 Wang, Z., Shi, W., and Liu, D., 2011, Continual erosion of bare rocks after the Wenchuan earthquake
172 and control strategies: *Journal of Asian Earth Sciences*, v. 40, p. 915-925, doi:
173 10.1016/j.jseaes.2010.07.004.
174 Yu, B., Ma, Y., and Wu, Y., 2013, Case study of a giant debris flow in the Wenjia Gully, Sichuan
175 Province, China: *Natural Hazards*, v. 65, p. 835-849, doi: 10.1007/s11069-012-0395-y.
176 Zhuang, J., You, Y., Chen, X., and Pei, L., 2012, Effect of infiltration and anti-scourability of
177 mixed-grain-sized, unconsolidated soil on debris flow initiation: *Bulletin of Soil and Water*
178 *Conservation*, v. 32, p. 43-47 (in Chinese).
179